

Aggregation of oriented anisotropic particles

Sasuke Miyazima

Department of Engineering Physics, Chubu University, Kasugai, Aichi 487, Japan

Paul Meakin

Central Research and Development Department, E.I. duPont de Nemours and Company, Inc., Experimental Station, Wilmington, Delaware 19898

Fereydoon Family

Department of Physics, Emory University, Atlanta, Georgia 30322

(Received 31 December 1986)

The diffusion-limited aggregation of oriented anisotropic particles is explored with use of computer simulations and scaling theory. The time-dependent cluster-size distribution (in both two- and three-dimensional systems) can be well represented by the dynamic scaling form for the cluster-size distribution $N_s(t) = s^{-2} f(s/S(t))$ where $N_s(t)$ is the number of clusters of size s at time t . The mean cluster size $S(t)$ diverges as $S(t) \sim t^z$. The value of the exponent z is found to agree with the mean-field Smoluchowski result $z = 1/(1-\gamma)$ in $d \geq d_c = 2$ dimensions, where d_c is the upper critical dimension, and γ is the exponent describing the dependence of the diffusion coefficient on the cluster mass. Below d_c , we find that our results agree with the expression $z = d/(2-d\gamma)$. At high particle densities, a crossover from two or three dimensions to one-dimensional behavior is observed.

I. INTRODUCTION

The formation of cluster by the aggregation of small objects and by growth processes is a subject of considerable interest and of practical importance in physics, chemistry, biology, medicine, and engineering.¹⁻³ The investigation of these processes has a long history and computer simulations have been used in this area for more than 20 years. Interest in nonequilibrium growth and aggregation processes has been heightened in recent years by the introduction of a simple diffusion-limited model for particle aggregation by Witten and Sander.⁴ The work of Witten and Sander stimulated the development of a diffusion-limited cluster-cluster aggregation model by Meakin⁵ and by Kolb *et al.*⁶ This model has been used to help develop a better understanding of both the structural and kinetic aspects of colloid aggregation. A widely used method of describing the aggregation process is the time dependence of the cluster-size distribution function $N_s(t)$.⁷ This quantity describes the number of clusters of size s at time t . It can be measured in experiments⁸⁻¹² or simulations¹³⁻¹⁶ and is the focus of the kinetic equation approach to coagulation.¹⁷

In this paper we shall discuss the aggregation of oriented particles to form linear structures (rods). A simple model for such a process has been developed in which the particles are able to join together only in the direction of orientation to form oriented rods which are also only able to aggregation via their ends.^{18,19}

We have in mind the aggregation of particles and/or clusters with induced dipole moments in an external field, the aggregation of magnetic particles in an external magnetic field, and aggregation or polymerization processes in an ordered liquid crystal. Aggregation in magnetic fluids

or ferrofluids is a particularly interesting example which is of considerable scientific and practical importance. A number of investigations of aggregation in ferrofluids have been carried out using both experimental,²⁰ analytical,^{21,22} or simulational^{23,24} methods.

A typical ferrofluid consists of single-domain magnetic particles, which are coated with a layer of long chain molecules to inhibit agglomeration, suspended in a fluid. The particle size of order of 10 nm is sufficiently small to maintain the Brownian motion. Magnetization is induced in each particle by external field according to Langevin theory. These magnetized particles become oriented in the magnetic field. The dipole-dipole interaction between two particles (or between particles and aggregates or between two linear aggregates) causes them to stick together if they diffuse sufficiently close to each other. Under typical conditions this aggregation process is essentially irreversible.

Here we shall investigate a similar process from the standpoint of the dynamical scaling theory.^{7,12-16} In our model the individual particles are represented by occupied lattice sites. At the start of a simulation the particles are distributed randomly on the lattice and follow random-walk paths on the lattice (to represent diffusion). If two particles or clusters come into contact (occupy nearest-neighbor lattice sites) and if they have the correct orientation with respect to each other (i.e., if their "ends" in the direction of orientation come into contact), they are joined permanently and continue to move as a single unit.^{5,6} If the sides of two particles or clusters come into contact, they do not stick. We consider only strong nearest-neighbor interactions in the direction of orientation. (Although dipole-dipole interactions are long range, the interaction energy will become smaller than kT at relatively

short distances and the detailed form of the interactions is not expected to modify the asymptotic scaling form for the aggregation dynamics.)

A variety of theoretical investigations of the aggregation of ferrofluids including a variety of Monte Carlo simulations^{23,24} have been carried out. In general, these investigations have been carried out using more realistic (and more elaborate) models have been directed towards developing a better understanding of static properties such as magnetization and structure (correlation functions). Here we are concerned primarily with the dynamic (kinetic) aspects of aggregation in these systems. In particular, we are interested in the asymptotic scaling behavior and its relationship to the behavior found previously in nonoriented systems.

It is interesting that there is a crossover from two- (or three-) dimensional behavior to one-dimensional behavior at high particle densities, because the diffusional motion is restricted to one dimension along the external field by the existence of other long rods.

In Sec. II the simulational method is discussed briefly. Results are given in Sec. III and the scaling theory in Sec. IV.

II. SIMULATION

Most of the simulations were carried out using 512×1024 ($w \times l$) square lattices and $64 \times 64 \times 512$ ($w \times w \times l$) cubic lattice with periodic boundary conditions. Initially $N_0 = \rho w^{d-1} l$ particles are placed randomly at N_0 sites on an $w^{d-1} l$ lattice. The diffusional motion of the particles and the clusters is represented by random walks on the lattice. In all of our simulations we assume that the diffusion coefficient D_s for clusters of mass s is given by $D_s = D_0 s^\gamma$ where D_0 is a constant. For the case $\gamma = 0$ (mass-independent diffusion coefficients), the time increased by $1/N(t)$ after each cluster has been moved where $N(t)$ is the total number of clusters at time t . For the case $\gamma \neq 0$, clusters are selected randomly as before. However, a random number x uniformly distributed in the range $0 < x < 1$ is generated and the cluster is moved only if $x < D_s/D_{\max}$, where D_s is the diffusion coefficient of the randomly selected cluster and D_{\max} is the maximum diffusion coefficient for any of the clusters in the system.

After each cluster has been randomly selected, the time is incremented by $1/D_{\max} N(t)$ whether the cluster is actually moved or not. In other words the time is incremented by $D_{\max}/n(t)$ for each attempted movement, where $n(t) = N(t)/w \times w \times l$. The direction of motion for the cluster is selected at random from all $4(2d)$ or $6(3d)$ possible directions on the lattice and the cluster is moved by one lattice unit in this direction providing that no overlap of clusters would occur from this move. If an overlap would occur, the cluster is not moved and a new cluster is randomly selected. After each cluster (or particle) has been moved, its perimeter is examined and the cluster is combined with any other cluster which contains an occupied site in the direction of orientation.

In this way the clusters which grow are linear and are orientated along the y axis (for $d = 2$) or along the z axis

(for $d = 3$). Simulations have also been carried out with anisotropic diffusion. However, the results from these numerations are not reported here. The number of long clusters oriented along the external field increases with time and the number of clusters with size s at time t , that is, the dynamical cluster-size distribution $N_s(t)$ is calculated. In most cases the results from a number of simulations (typically 10–100) were averaged to reduce statistical uncertainty.

III. RESULTS

In the two-dimensional case, 10 000 particles were distributed on square lattices of 512×1024 sites corresponding to a density (ρ) of 0.019. Three kinds of diffusion coefficients $D(s) \sim s^0$, $s^{-0.5}$, and $s^{-1.0}$ were considered and the dependence of cluster-size distribution on the exponent γ was examined.

Figures 1(a)–1(d) show the results obtained from two-dimensional simulations using mass independent diffusion coefficients ($\gamma = 0$). Figure 1(a) shows the total number of clusters $N(t)$ as a function of time. At long times the dependence of $\ln[N(t)]$ on $\ln(t)$ is linear with a slope close to -1 . Similarly Fig. 1(b) shows the dependence of the mean (weight average) cluster size $S(t)$ on t , which is defined by

$$S(t) = \sum_s s^2 N_s(t). \quad (1)$$

Our results indicate that, asymptotically, $S(t) \sim t^z$ and that the exponent z is a value of approximately 1.0. (See Sec. IV.) Figure 1(c) shows the time-dependent cluster-size distribution $N_s(t)$ versus the time t where each curve corresponds to clusters of size $s = 1, 2, 3, 4, 10, 19-20, 38-40$, and $75-80$ occupied lattice site. The slope of the curves at long times is about -1.75 . The time-dependent cluster-size distribution versus the cluster size s is shown in Fig. 1(d) at times $t = 2.44, 6.56, 17.67, 47.58, 128.1, 344.8, 928.4, 2499$, and 6729 . The slope of common tangent is -2.0 .

Similar results are given in Fig. 2(a)–2(d) for the case $\gamma = -0.5$ and Figs. 3(a)–3(d) for the case $\gamma = -1.0$. Figures 2(a) and 3(a) describe the total number of clusters $N(t)$ as a function of time. The slopes at long times are $-1, -0.64$, and -0.5 for $\gamma = 0, -0.5$, and -1.0 , respectively. Figures 2(b) and 3(b) show the average cluster sizes as a function of t for $\gamma = -0.5$ and -1.0 , respectively. The slopes at long times in these log-log plots are $1, 0.65$, and 0.5 for $\gamma = 0, -0.5$, and -1.0 , respectively. These results show that $S(t) \sim t^z$ and $N(t) \sim t^{-z}$ where the exponent z has values of approximately $1, \frac{2}{3}$, and $\frac{1}{2}$ for $\gamma = 0, -\frac{1}{2}$, and -1 , respectively. This result suggests that $z = 1/(1-\gamma)$. Figures 2(c) and 3(c) show the time dependence of the number of clusters or various sizes obtained during simulations with $\gamma = -0.5$ and -1 . For the case $\gamma = 0$ these curves converge to a common curve at long times; for $\gamma < 0$ the behavior is qualitatively different and there is a common tangent to the curves with a slope of -1.22 for $\gamma = -\frac{1}{2}$ and -0.97 for $\gamma = -1.0$.

The cluster-size distributions obtained at several times during the simulations used to generate the results shown in Figs. 2(c) and 3(c) are shown in Figs. 2(d) and 3(d). In all three cases ($\gamma=0$, -0.5 [Fig. 2(d)], and -1.0 [Fig. 3(d)]) the slope of the common tangent in these log-log plots is close to -2.0 .

Figures 4(a) and 4(b) show some results obtained from

two-dimensional simulations carried out using 8000 particles (occupied lattice sites) on 512×512 lattices. Figure 4(a) shows a simulation carried out with $\gamma=0$ at the stage where the mean cluster size (S) had reached 21.2 sites per cluster. Figure 4(b) shows similar results obtained from a simulation carried out with $D(s) \sim s^{-1}$ at the stage where $S=20.2$.

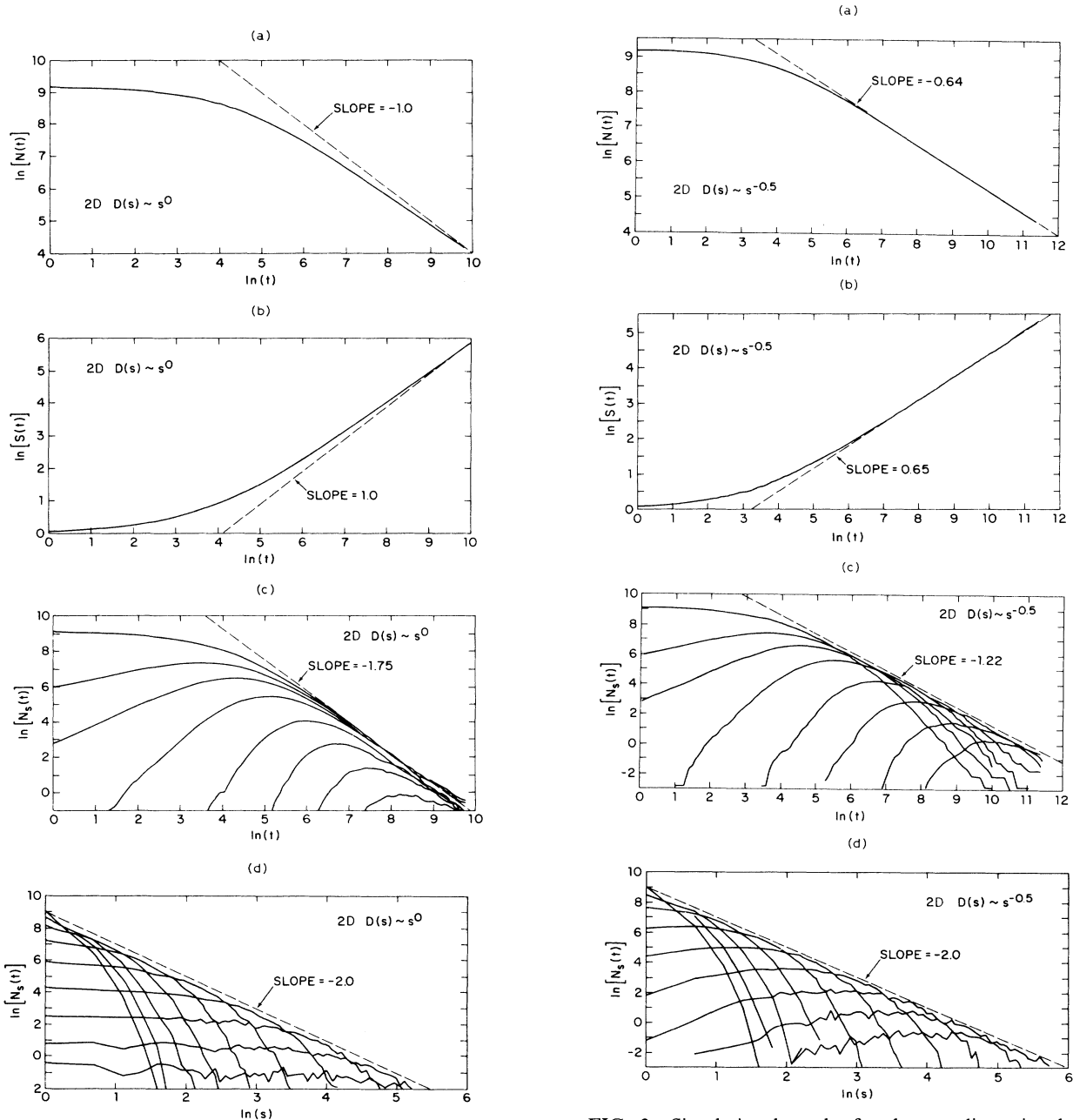


FIG. 1. Simulation results for the two-dimensional square lattice (512×1024) are given for $\gamma=0$. (a) The total number of clusters vs the time, (b) the average cluster size vs the time, (c) the dynamical cluster-size distribution vs the time for $s=1, 2, 3, 4, 10, 19-20, 38-40$, and $75-80$, and (d) the dynamical cluster-size distribution vs cluster size s at $t=2.44, 6.56, 17.07, 47.58, 128.1, 344.8, 978.4, 2499$, and 6729 .

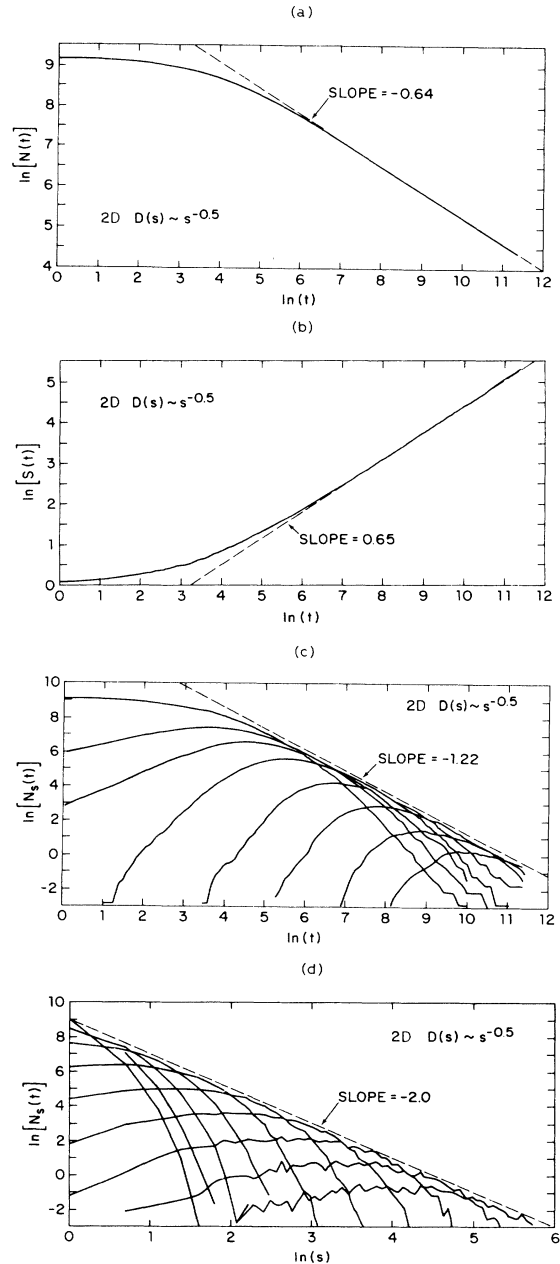


FIG. 2. Simulation results for the two-dimensional square lattice (512×1024) are given for 10 000 particles and $\gamma = -0.5$. (a) The total number of clusters vs the time, (b) the average cluster size vs the time, (c) the dynamical cluster-size distribution vs the time for $s=1, 2, 3, 5, 10, 19-20, 38-40$, and $75-80$, and (d) the dynamical cluster-size distribution vs cluster size s at $t=2.82, 8.91, 28.2, 89.1, 282, 891, 2820, 8910, 28200$, and 89100 .

In the three-dimensional case, 10 000 particles were initially distributed on the cubic lattice of $64 \times 64 \times 512$ with the cyclic boundary condition, so that $\rho = 0.0048$. Results were obtained using three different diffusion coefficient exponents ($\gamma = 0, -0.5$, and -1.0). Figure 5 shows the results which were obtained for the case $\gamma = -1.0$. Figure 5(a) shows the dependence of the total number of clusters

(including single-particle clusters) on the time. At long times we find that $N(t) \sim t^{-z}$ where the exponent z has a value of about -0.50 . Similarly Fig. 5(b) shows that the mean cluster size $S(t)$ depends on time (in the long-time limit) according to $S(t) \sim t^z$ ($z \approx 0.50$). Similar results obtained from simulations carried out with $\gamma = 0$ and $\gamma = -1$ indicate that $S(t) \sim t^z$, $N(t) \sim t^{-z}$ where the exponent z has a value given by $z = 1/(1 - \gamma)$.

Figures 5(a) and 5(d) show the time-dependent cluster-size distributions obtained from the $3d$ simulations carried out with $\gamma = -1.0$. Figure 5(c) shows the time dependence of the number of clusters of size $s = 1, 2, 3, 5, 10, 19-20$, and $38-40$.

For large clusters (long rods) these curves have a bell

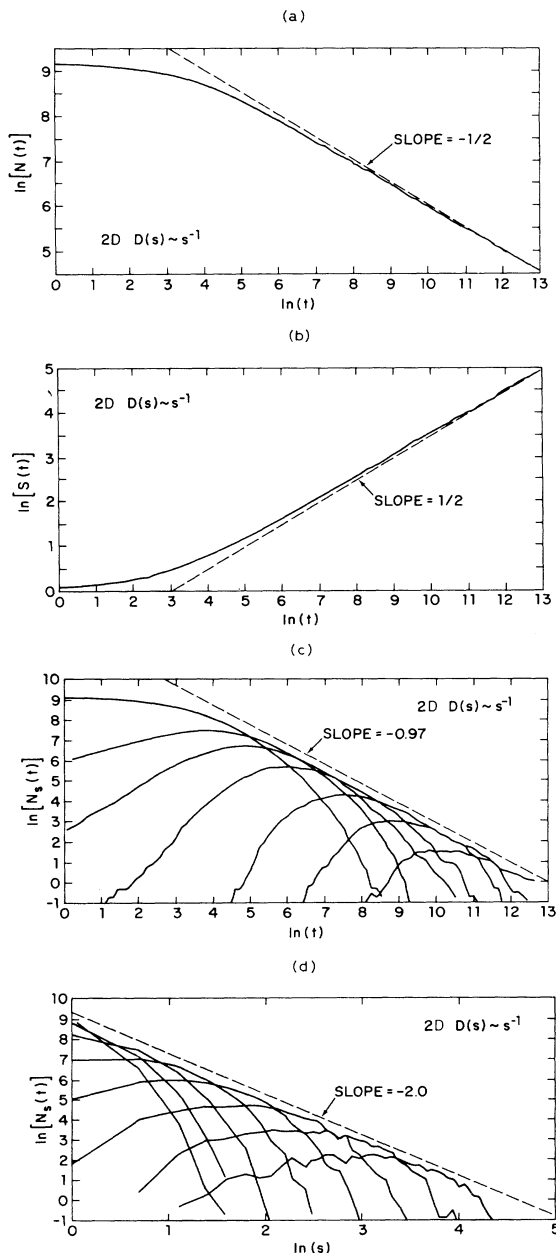


FIG. 3. Simulational results for the two-dimensional square lattice (512×1024) are given for 10 000 particles and $\gamma = 1$. (a) total number of clusters vs the time, (b) the average cluster size vs the time, (c) the dynamical cluster-size distribution vs the time for $s = 1, 2, 3, 5, 10, 19-20$, and $38-40$, and (d) the dynamical cluster-size distribution vs cluster size s at $t = 3.26, 12.10, 44.95, 167.0, 620.1, 2304, 8556$, and $31\,782$.

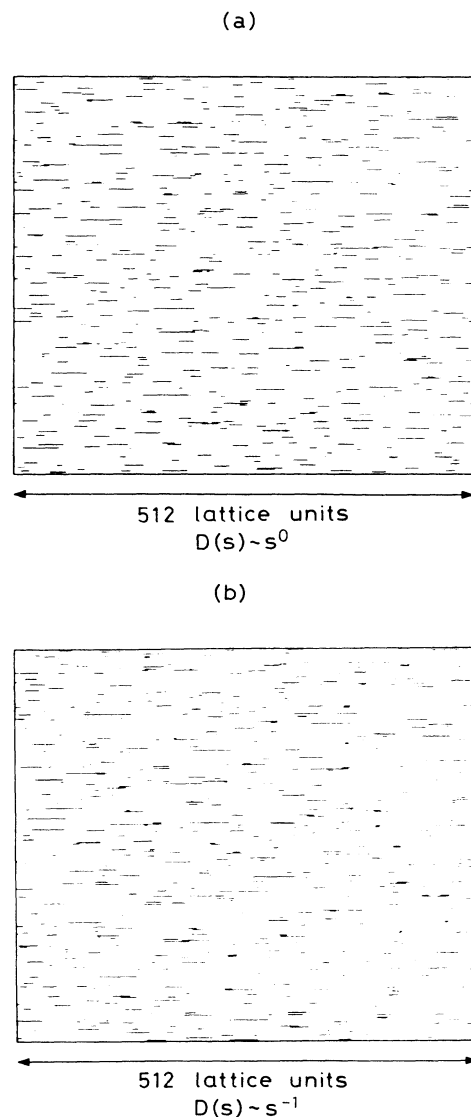


FIG. 4. Patterns of formed linear rods in the 512×512 square lattice. Initially 8000 particles are distributed and in (a) the average cluster size is 20.19 and $\gamma = -1$ and in (b) the average cluster size is 21.16 and $\gamma = 0$.

shape and their common tangent has a slope of about -1.0 . For $\gamma = -0.5$ the common tangent has a slope of about -1.32 and for $\gamma = 0$ the time dependence of the number of clusters of all sizes converges to a single curve with an exponent of about -1.75 . Figure 5(d) shows the time-dependent cluster-size distributions (for $\gamma = -1$) obtained at several different times during the simulations.

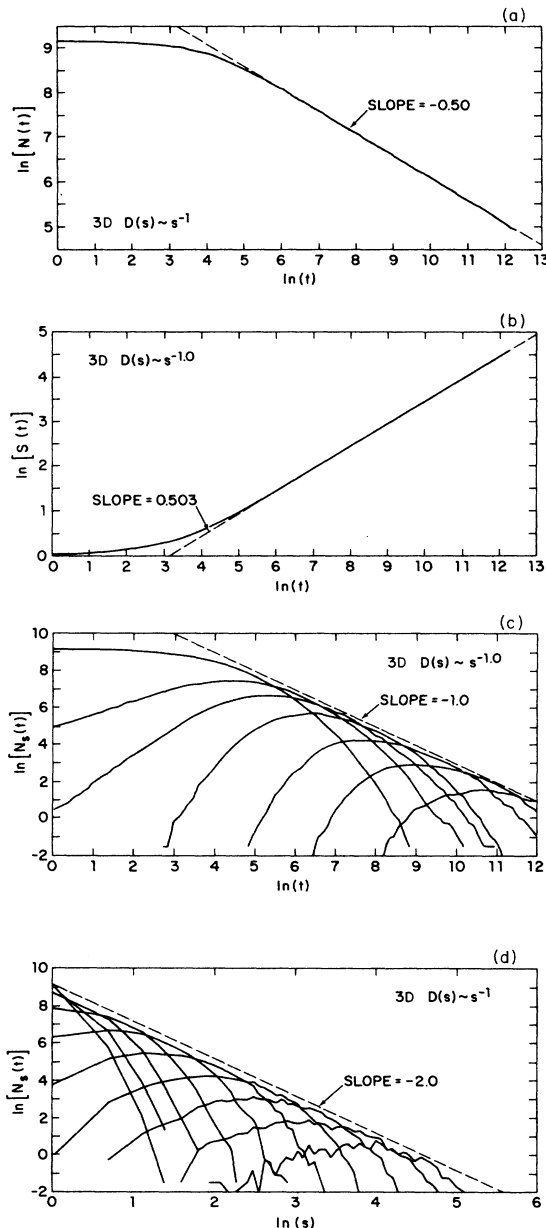


FIG. 5. Simulation results for the three-dimensional cubic lattice ($64 \times 64 \times 512$) model with $\gamma = -1.0$ and 10 000 particles. (a) The total number of clusters vs the time, (b) the average cluster size vs the time, (c) the dynamical cluster-size distribution vs the time for $s = 1, 2, 3, 5, 10, 19-20$, and $38-40$, and (d) the dynamical cluster-size distribution vs cluster size s at times 3.06, 10.61, 36.8, 127.4, 441.6, 1530, 5303, 18 280, and 67 300.

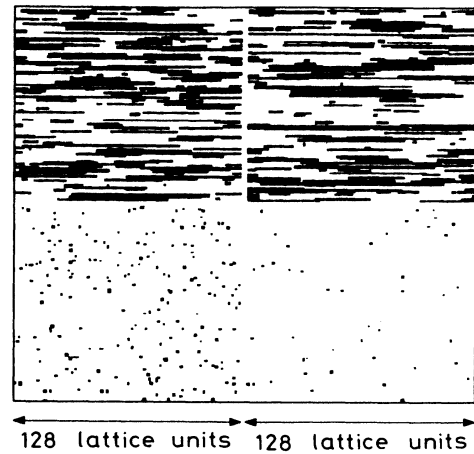


FIG. 6. A "snapshot" of a simulation in which 10 000 sites on a 128^3 -site cubic lattice were initially filled at random to represent particles. The two upper parts of the figure show projections onto the x - z and y - z planes at the stage where the mean cluster size $[S(t)]$ has reached a value of 40. The lower left-hand corner shows a projection onto the x - y plane and the lower right-hand corner shows a cross section perpendicular to the z axis (the axis of anisotropy). In this simulation the diffusion coefficient exponent γ was given a value of 0.

For these simulations (and for similar simulations carried out using diffusion coefficient exponents γ of -0.5 , and 0) the slope of the common tangent to these curves is -2.0 .

Figure 6 shows a "snapshot" of a simulation carried out using 10 000 particles on a cubic lattice ($128 \times 128 \times 128$) with time-dependent cluster diffusion coefficients $[D(s) \sim s^0]$ at the stage where the mean cluster has reached about 40. The top part of the figures shows projection of the system onto the x - z and y - z planes. The lower left-hand corner shows the projection onto the x - y plane and the lower right-hand corner shows a cross section parallel to the x - y plane.

In order to study the effects of particle concentration on the dynamics of the aggregation process, we have carried out a series of 2D simulations with increasing density. As an example, in Fig. 7 we show the results for $\gamma = -1$. In the low density limit ($\rho = 0.019$) $S(t)$ is found to grow

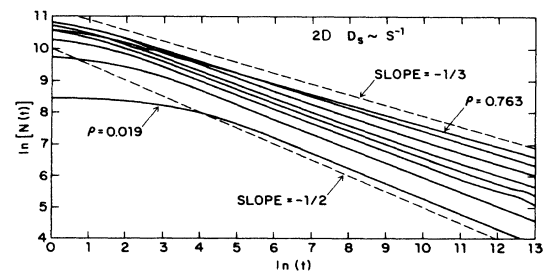


FIG. 7. Dependence on $\ln[S(t)]$ and $\ln(t)$ obtained from two-dimensional simulation carried out with $\gamma = -1.0$ at various densities.

with a power of $z = \frac{1}{2}$, corresponding to a $2d$ behavior with $z = 1/(1-\gamma)$. However, as ρ increases, z decreases and for the highest value of ρ ($=0.763$) $S(t)$ grows as $t^{1/3}$ corresponding to $z = \frac{1}{3}$ in agreement with a $1d$ behavior [see Eq. (7) in Sec. IV].

As for the exponent γ of diffusion constant, it is apparent from the numerical results that $\gamma \sim 0$ is the critical value, at which the shape of $N_s(t)$ changes from monotonically decreasing function to a bell-shaped curve.

IV. SCALING THEORY AND THE RATE EQUATION APPROACH

The basic assumption in the dynamic scaling theory for the cluster-size distribution is that there exists only one diverging characteristic cluster size, S , in the system.^{7,12-16} Usually this typical cluster size is taken to be the mean cluster size which is defined by (1). The assumption that the density of the system ρ is a fixed constant independent of time leads to the following general scaling form for the cluster-size distribution:⁷

$$N_s(t) = s^{-2} f(s/S(t)), \quad (2)$$

where $f(x)$ is a scaling function that depends on details of the aggregation process. This scaling description has been found to generally apply to irreversible aggregation,^{7,14,15} reversible aggregation,¹⁶ disaggregation,²⁵ and to experiments on gold colloids.²⁶

In irreversible processes the mean cluster size grows with time.⁵⁻⁷ On the basis of the dynamic scaling description,^{7,12-16} assume that S diverges with a power of t and define the dynamic scaling exponent z from the following relation:

$$S(t) \sim t^z. \quad (3)$$

The exponent z has been determined for various coagulation processes and is found to depend on details of the process.

The coagulation process can also be discussed in terms of the Smoluchowski kinetic equation.^{17,18} In this approach a rate equation is used for calculating $N_s(t)$ and the dynamics of the process is determined by the reaction kernel K_{ij} which gives the rate at which a cluster of size i joins to a cluster of size j to form a cluster of size $i+j$. Assuming that the Smoluchowski equation has the same scale-invariance property as the cluster-size distribution, it is known that if $K_{i\lambda j\lambda} = \lambda^{2\omega} K_{ij}$, the exponent z defined in (3) is given by

$$z = 1/(1-2\omega), \quad \omega < \frac{1}{2}. \quad (4)$$

For diffusive coagulation it can be shown that K_{ij} is a product of a collision cross-section term $(R_i + R_j)^{d-2}$ and a diffusion coefficient $(D_i + D_j)$, where R_i and D_i are the radius and the diffusion constant of a cluster of size i , respectively. In the present problem the collision cross section is independent of the cluster mass and since $D_i \sim i^\gamma$, K_{ij} is given by

$$K_{ij} \sim i^\gamma + j^\gamma \quad (5)$$

and

$$z = 1/(1-\gamma). \quad (6)$$

Due to the nature of the approximation inherent in the derivation of the Smoluchowski equation, the above result represents a mean-field approximation to the dynamic exponent z . Thus we expect Eq. (6) for z to hold in dimensions $d \geq d_c$ where d_c is the upper critical dimension above which fluctuations become relevant and the mean-field approximation breaks down.

In order to test the mean-field result obtained from the Smoluchowski equation, we have compared the values of z obtained from the simulations with (6). We find that the simulation results for various values of γ are in excellent agreement with (6) in dimensions $d \geq 2$, but strongly disagree with it in one dimension. This result indicates that the upper critical dimension for this coagulation process is $d_c = 2$ and the Smoluchowski equation mean-field result breaks down in $d \geq 2$.

Recently Kang *et al.*²⁷ have used some plausible, but heuristic, arguments to calculate the exponent z below $d_c = 2$ for the particle coalescence model which is equivalent to our model in one dimension. They find that z is given by

$$z = d/(2-d\gamma). \quad (7)$$

Our simulation results for various γ are again in excellent agreement with this prediction in one dimension.

To evaluate the validity of scaling theory we have checked the data collapse in the plot of $\ln[s^2 N_s(t)]$ versus $\ln[s/S(t)]$ for $\gamma = -1.0$ as shown in Figs. 8(a) and 8(b),

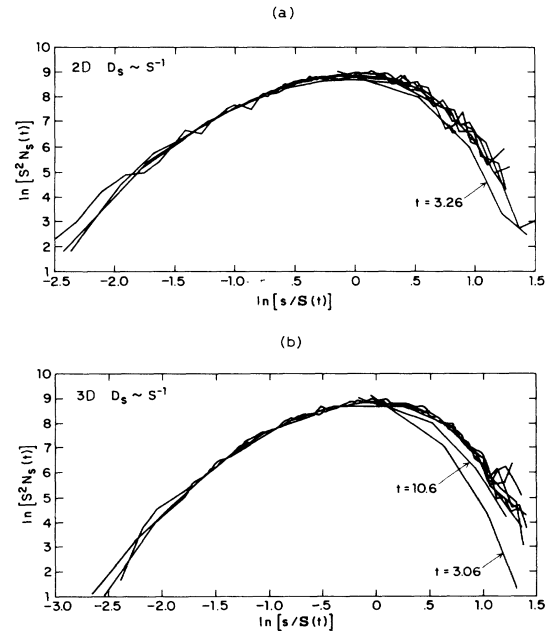


FIG. 8. Test of the scaling form given in Eq. (2) using the results from two-dimensional [Fig. 5(a)] and three-dimensional simulations. In both cases the diffusion coefficient exponent (γ) has a value of -1.0 . Both figures show a good data collapse except at short times.

where the data collapse is very good except at short times $t = 3.26$ ($2d$) and $t = 3.06$ and 10.6 ($3d$). The satisfactory data collapse indicates that Eq. (2) is valid except at very short times.

V. CONCLUSION

In this paper we studied a generalization of the coagulation process in which oriented particles were allowed to aggregate and form linear structures (rods). We investigated the dynamics of aggregation through the time-dependent properties of the cluster-size distribution and its moments. By using a scaling plot, the data for the cluster-size distribution at different times was found to collapse to a single curve indicating agreement with the dynamic scaling theory.⁷ The mean cluster size and the total number of particles were found to scale with time with the exponent z .^{7,12-16} The value of z in $d = 2$ and 3 were found to be in agreement with the predictions of the mean-field Smoluchowski equation. This is consistent with an upper critical dimension $d_c = 2$ for the coagulation process. Due to the presence of fluctuations, the exponent z was found to be different from its mean-field value in

$d = 1$, but in agreement with Eq. (7). At higher concentrations we observed a crossover from a two- or three-dimensional behavior to a one-dimensional behavior. This is due to the anisotropic nature of the aggregation which does not allow for the clusters to diffuse through one another at high concentrations and the final process becomes dominated by one-dimensional-type aggregation.

ACKNOWLEDGMENTS

One of us (S.M.) thanks Chubu University for financial support during his stay at the Center for Polymer Studies in Boston University. He thanks Professor H. E. Stanley for various discussions and his hospitality. F.F. acknowledges support from the Office of Naval Research and the donors of The Petroleum Research Fund, administered by the American Chemical Society. He would also like to thank John Deutch for his hospitality and support at the Massachusetts Institute of Technology. This work was accomplished mainly during S.M.'s stay at the Center for Polymer Studies of Boston University and F.F.'s stay at the Department of Chemistry, Massachusetts Institute of Technology, Cambridge, MA.

¹See, e.g., *Kinetics of Aggregation and Gelation*, edited by F. Family and D. P. Landau (North-Holland, Amsterdam, 1984).

²*On Growth and Forms*, edited by H. E. Stanley and N. Ostrowsky (Martinus Nijhoff, Dordrecht, The Netherlands, 1986).

³K. Friedlander, *Smoke, Dust and Haze: Fundamentals of Aerosol Behavior* (Wiley, New York, 1977).

⁴T. A. Witten, Jr. and L. M. Sander, *Phys. Rev. Lett.* **47**, 1400 (1981).

⁵P. Meakin, *Phys. Rev. Lett.* **51**, 1119 (1983).

⁶M. Kolb, R. Botet, and R. Jullien, *Phys. Rev. Lett.* **51**, 1123 (1983).

⁷T. Vicsek and F. Family, *Phys. Rev. Lett.* **52**, 1669 (1984).

⁸R. B. Husar and K. T. Whitby, *Environ. Sci. Technol.* **9**, 279 (1975).

⁹G. Gartrell, Jr. and S. K. Friedlander, *Atmos. Environ.* **9**, 279 (1975).

¹⁰G. K. von Schulthess, G. B. Benedek, and R. W. deBlois, *Macromolecules* **13**, 939 (1980).

¹¹J. M. Soler, N. Garcia, O. Echt, K. Sattler, and E. Ricknagel, *Phys. Rev. Lett.* **49**, 1857 (1982).

¹²K. Sattler, in *Festkörperprobleme*, Vol. XXIII of *Advances in Solid State Physics*, edited by P. Grosse (Vieweg, Braunschweig, 1983), p. 1.

¹³M. Kolb, *Phys. Rev. Lett.* **53**, 1653 (1984).

¹⁴F. Family, P. Meakin, and T. Vicsek, *J. Chem. Phys.* **83**, 4144

(1985).

¹⁵P. Meakin, T. Vicsek, and F. Family, *Phys. Rev. B* **31**, 564 (1985).

¹⁶F. Family, P. Meakin, and J. M. Deutch, *Phys. Rev. Lett.* **57**, 727 (1986).

¹⁷M. von Smoluchowski, *Z. Phys.* **17**, 585 (1916); *Z. Phys. Chem.* **92**, 129 (1918); see also T. Vicsek and F. Family, R. Ziff, and M. E. Ernst and E. M. Hendriks, in Ref. 1.

¹⁸R. L. Drake, in *Topics in Current Aerosol Research*, edited by G. M. Hidy and J. R. Brock (Pergamon, New York, 1972), Vol. III, p. 201.

¹⁹P. G. deGennes and P. A. Pincus, *Phys. Kondens. Mater.* **11**, 189 (1970).

²⁰For a bibliography on ferrofluids, see M. Zahn and K. E. Shenton, *IEEE Trans. Magn.* **16**, 387 (1980).

²¹P. C. Jordon, *Mol. Phys.* **25**, 961 (1973).

²²J. B. Hayter and R. Pynn, *Phys. Rev. Lett.* **49**, 1103 (1982).

²³R. W. Chantrell, A. Bradbury, J. Popplewell, and S. W. Charles, *J. Appl. Phys.* **53**, 2742 (1982).

²⁴S. Hess, J. B. Hayter, and R. Pynn, *Mol. Phys.* **53**, 1527 (1984).

²⁵A. Kersfin (unpublished).

²⁶D. Weitz and M. Oliveria, *Phys. Rev. Lett.* **52**, 1433 (1984).

²⁷K. Kang, S. Redner, P. Meakin, and F. Leyvraz, *Phys. Rev. A* **33**, 1171 (1986).